arXiv:2009.01000v1 [quant-ph] 2 Sep 2020

Discriminating qubit amplitude damping channels

Milajiguli Rexiti*
School of Science and Technology, University of Camerino, 62032 Camerino, Italy

Stefano Mancini†
School of Science and Technology, University of Camerino, 62032 Camerino, Italy
and INFN-Sezione di Perugia, 06123 Perugia, Italy
(Dated: September 3, 2020)

We address the issue of the discrimination between two-qubit amplitude damping channels by exploring several strategies. For the single-shot, we show that the excited state does not always give the optimal input, and that side entanglement assistance has limited benefit. On the contrary, feedback assistance from the environment is more beneficial. For the two-shot, we prove the in-utility of entangled inputs. Then focusing on individual (local) measurements, we find the optimal adaptive strategy.

I. INTRODUCTION

A quantum channel is a linear stochastic (precisely a linear, completely positive and trace-preserving) map on the set of density operators [1]. As such, it can describe any physical process. It is often essential to distinguish between two (or even more) physical processes. Hence the issue of quantum channel discrimination becomes pervasive well beyond the boundary of information theory [2–6]. Quite generally, channel discrimination is a challenging task [7–10]. In fact, although it can be traced back to the (somehow old problem of) states discrimination [11, 12], it involves a double optimization: on the output measurement and the input state. Recently, bounds on the error probability were found for general strategies [13, 14].

Among quantum channels, the amplitude damping plays a prominent role as it describes the energy loss of a system, which is the most common effect occurring in an open system. As a matter of fact, this channel is often invoked as an example when dealing with discrimination (see e.g. [13, 14]). However, a systematic and thorough study of amplitude damping channel discrimination starting from dimension two is still lacking. Here we address this issue and unveil several unexpected results. For one-shot discrimination, the optimal input state turns out to not always be the excited state. Furthermore, side entanglement has a limited benefit because of a limited parameter region where it brings improvement and the smallness of such improvement. In contrast, feedback assistance from the environment results more beneficial. By such feedback, we mean the possibility to access the environment, measure it and then use this (classical) information to adjust the state of (or the measurement process in) the main system according to the desired goal [15]. Additionally, we prove that entangled inputs are not useful for two-shot, although collective measurement can give the minimum error probability. Then, restricting the attention to individual measurements, we find the optimal adaptive strategy (useful for a complete LOCC strategy [16]).

The paper is organized in two main Sections. Sec.II is devoted to one-shot discrimination. In Subsec.II A the optimal input is found. In Subsec.II B side entanglement is considered. Feedback assistance model is presented in Subsec.II C. Then, Sec.III is devoted to two-shot discrimination.

*Electronic address: milajiguli.milajiguli@unicam.it
†Electronic address: stefano.mancini@unicam.it

In Subsec.III A the optimal input is found when also collective measurements are allowed. The optimal adaptive strategy for individual measurements is devised in Subsec.III B. Finally, in Sec.IV conclusions are drawn.

II. ONE-SHOT DISCRIMINATION

It is customary to consider the amplitude damping channel as coming from the unitary interaction of the system with the environment generated by

$$H = \eta \left(a^\dagger b + a b^\dagger \right), \tag{1}$$

where $a, a^\dagger$ (res. $b, b^\dagger$) are the ladder operators of the system (resp. environment).

For a qubit system and qubit environment, in the computational basis $\{|00\rangle, |01\rangle, |10\rangle, |11\rangle\}$ we have

$$H = \begin{pmatrix} 0 & 0 & 0 & 0 \\ 0 & 0 & \eta & 0 \\ 0 & \eta & 0 & 0 \\ 0 & 0 & 0 & 0 \end{pmatrix}, \tag{2}$$

and then the corresponding unitary $U = e^{-iH}$ reads

$$U = \begin{pmatrix} 1 & 0 & 0 & 0 \\ 0 & \cos\eta & -i\sin\eta & 0 \\ 0 & -i\sin\eta & \cos\eta & 0 \\ 0 & 0 & 0 & 1 \end{pmatrix}. \tag{3}$$

The map on the system's states can be written as

$$\mathcal{N}(\rho) = K_0 \rho K_0^\dagger + K_1 \rho K_1^\dagger, \tag{4}$$

where the Kraus operators are given by

$$K_0 = \langle 0|U|0\rangle = \begin{pmatrix} 1 & 0 \\ 0 & \cos\eta \end{pmatrix}, \tag{5}$$

$$K_1 = \langle 1|U|0\rangle = \begin{pmatrix} 0 & -i\sin\eta \\ 0 & 0 \end{pmatrix}, \tag{6}$$

with the bra-ket taken on the environment. The quantity $\sin^2\eta$ represents the decay probability ($\eta \in [0, \frac{\pi}{2}]$).

A. Optimal input

Let us analyze the distinguishability of two amplitude damping channels characterized by parameters η_0 and η_1. By referring to Fig.1, we assume that each one acts with probability $P_0 = P_1 = 1/2$ on an input state

$$|\psi\rangle = \sqrt{1-x}\,|0\rangle + e^{-i\varphi}\sqrt{x}\,|1\rangle, \tag{7}$$

where $x \in [0,1]$ and $\varphi \in [0, 2\pi)$. Without loss of generality, we take $\eta_0 > \eta_1$. We can also set $\varphi = 0$, because of the symmetric action of $\mathcal{N}$ with respect to the z axis in the Bloch sphere.

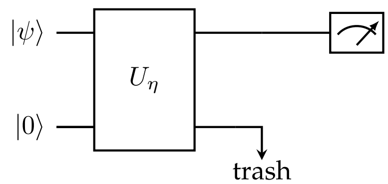

Figure 1: Schematic representation of the channel discrimination through unitary dilation. One has to determine whether U_{η_0} or U_{η_1} acted by controlling only the main system (top line).

According to (3), we obtain

$$U_{\eta_i} |\psi\rangle |0\rangle \;=\; \sqrt{1-x}\,|00\rangle + \sqrt{x}\,(-i\sin\eta_i\,|01\rangle + \cos\eta_i\,|10\rangle)\,, \qquad i=0,1. \tag{8}$$

Consequently, the output state of the channel reads

$$\begin{aligned}\rho_i = &\left(1-x+x\sin^2\eta_i\right)|0\rangle\langle 0| + \sqrt{x(1-x)}\cos\eta_i\,|0\rangle\langle 1| \\ &+ \sqrt{x(1-x)}\cos\eta_i\,|1\rangle\langle 0| + x\cos^2\eta_i\,|1\rangle\langle 1|\,, \qquad i=0,1.\end{aligned} \tag{9}$$

So the problem of channel discrimination is now translated into the discrimination between two mixed states, ρ_0 and ρ_1, each occurring with probability $1/2$. To this end, it is known that the optimal measurement is given by the observable $\rho_0-\rho_1$ [1]. Denoting by $|v_0\rangle$ and $|v_1\rangle$ its (normalized) eigenvectors corresponding respectively to positive and negative eigenvalues, we obtain

$$\begin{aligned}P_0(0) \equiv \langle v_0|\rho_0|v_0\rangle = &\frac{(\gamma-2\sqrt{1-\gamma^2})}{4(1-\gamma^2)\left[4(1-\gamma^2)+(\gamma-2\sqrt{1-\gamma^2})^2\right]} \\ &\times\Big\{12-27\gamma^2+16\gamma^4+8\gamma\sqrt{1-3\gamma^2+2\gamma^4}\cos\eta_0-(4-5\gamma^2)\cos(2\eta_0) \\ &-8\cos\eta_0\left[2\sqrt{1-2\gamma^2}(1-\gamma^2)+\gamma\sqrt{1-\gamma^2}\cos\eta_0\right]+8(1-\gamma^2)\cos^2\eta_0\Big\}, \quad \text{for} \quad \gamma<\frac{1}{\sqrt{2}},\end{aligned} \tag{10a}$$

$$P_0(0) \equiv \langle v_0|\rho_0|v_0\rangle = \sin^2\eta_0, \quad \text{for} \quad \gamma\geq\frac{1}{\sqrt{2}}, \tag{10b}$$

and

$$\begin{aligned}P_1(1) \equiv \langle v_1|\rho_1|v_1\rangle = &\frac{1}{4(1-\gamma^2)\left[4(1-\gamma^2)+(\gamma+2\sqrt{1-\gamma^2})^2\right]} \\ &\times\Big\{12-27\gamma^2+16\gamma^4+8\gamma\sqrt{1-3\gamma^2+2\gamma^4}\cos\eta_1-(4-5\gamma^2)\cos(2\eta_1) \\ &+8\cos\eta_1\left[2\sqrt{1-2\gamma^2}(1-\gamma^2)+\gamma\sqrt{1-\gamma^2}\cos\eta_1\right]+8(1-\gamma^2)\cos^2\eta_1\Big\}, \quad \text{for} \quad \gamma<\frac{1}{\sqrt{2}},\end{aligned} \tag{11a}$$

$$P_1(1) \equiv \langle v_0|\rho_0|v_0\rangle = \cos^2\eta_1, \quad \text{for} \quad \gamma\geq\frac{1}{\sqrt{2}}, \tag{11b}$$

where

$$\gamma \equiv \gamma(\eta_0,\eta_1) \equiv \cos\eta_0 + \cos\eta_1. \tag{12}$$

Note that for the input state $|\psi\rangle$ the optimal value of x results

$$x = \frac{1}{2-2\gamma^2}, \quad \text{for} \quad \gamma < \frac{1}{\sqrt{2}}, \tag{13a}$$

$$x = 1, \quad \text{for} \quad \gamma \geq \frac{1}{\sqrt{2}}. \tag{13b}$$

This means, interestingly, that the optimal input state is not always the excited state $|1\rangle$ as one would expect (just because it is considered as the most sensitive state to the damping action).

Then, the probability of success in discriminating between two mixed states, ρ_0 and ρ_1, each occurring with probability $1/2$, is given by

$$P_{succ} = \frac{1}{2}P_0(0) + \frac{1}{2}P_1(1). \tag{14}$$

This turns also out to be [1]

$$P_{succ} = \frac{1}{2}\left(1 + \frac{1}{2}\left\|\rho_0 - \rho_1\right\|_1\right), \tag{15}$$

where

$$\|T\|_1 \equiv \mathrm{Tr}\sqrt{T^\dagger T}. \tag{16}$$

Finally, inserting (10) and (11) into (14) (or equivalently using (9) into (15)), yields

$$P_{succ} = \frac{1}{4}\left(2 + \frac{\cos\eta_1 - \cos\eta_0}{\sqrt{1-\gamma^2}}\right), \quad \gamma < \frac{1}{\sqrt{2}}, \tag{17a}$$

$$P_{succ} = \frac{1}{2}\left(\sin^2\eta_0 + \cos^2\eta_1\right), \quad \gamma \geq \frac{1}{\sqrt{2}}. \tag{17b}$$

B. Side entanglement

Consider the usage of side entanglement according to the model of Fig.2.

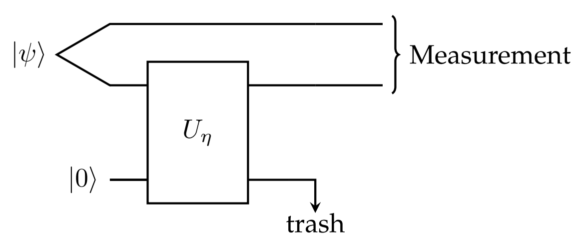

Figure 2: Model for channel discrimination exploiting entanglement between the input system and an accessible reference system.

Let $|\Psi\rangle = \sqrt{1-x}\,|01\rangle + \sqrt{x}\,|10\rangle$ be an entangled state between the reference system and the channel's input. Then, we have to distinguish between the following two states at the measurement stage:

$$\begin{aligned}\mathrm{Tr}_E\left\{(I\otimes U_{\eta_i})\,|\Psi\rangle\,|0\rangle\,\langle 0|\,\langle\Psi|\,(I\otimes U_{\eta_i})^\dagger\right\} &= \cos^2\eta_i(1-x)|01\rangle\langle 01| + x|10\rangle\langle 10| \\ &+ \sqrt{x(1-x)}\cos\eta_i\left(|01\rangle\langle 10| + |10\rangle\langle 01|\right) \\ &+ (1-x)\sin^2\eta_i|00\rangle\langle 00|, \qquad i = 0,1,\end{aligned} \tag{18}$$

where the unitaries are as in (3).

The success probability (15) for the states in (18) leads to a cumbersome function $P_{succ}(\eta_0,\eta_1,x)$ which is not reported. Then, we show in Fig.3 the difference

$$P_{succ}(\eta_0,\eta_1,x^*) - P_{succ}(\eta_0,\eta_1,0), \tag{19}$$

where

$$x^*(\eta_0,\eta_1) := \mathrm{argmax}_x \; P_{succ}(\eta_0,\eta_1,x). \tag{20}$$

This latter quantity gives the optimal amount of entanglement and is shown in Fig.4.

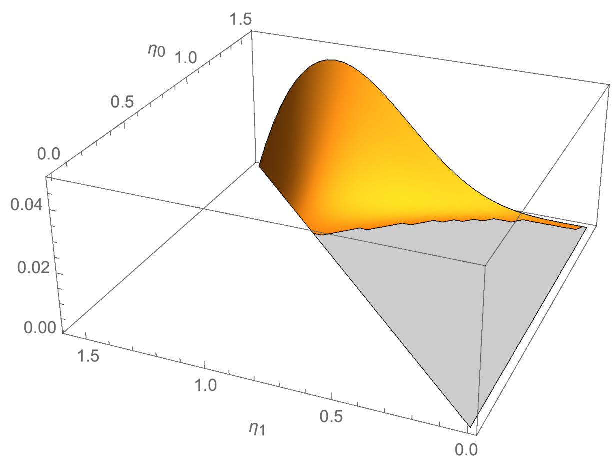

Figure 3: Difference between success probability computed at optimal x and $x = 0$ ((19)) vs η_0 and η_1.

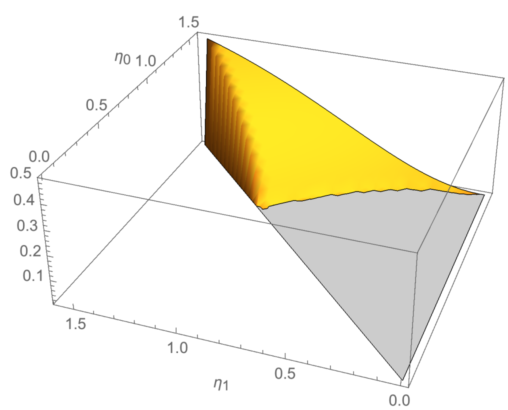

Figure 4: Optimal value of x ((20)) vs η_0 and η_1.

Fig.3 shows that the improvement due to the side entanglement is relatively tiny. Moreover, it does not occur in all parameters' region. This is in contrast to what happens, e.g., for Pauli channels [10], and it should be ascribed to the amplitude damping channel's asymmetric action on the space of states (which also gives rise to its non-unitality). Nevertheless, the parameters' region where entanglement is useful is consistent with the entanglement breaking property [9], which shows up for $\eta_0 > \frac{\pi}{4}$. It is also interesting to note from Fig.4 that a small amount of entanglement is more effective (x never reaches the maximum $\frac{1}{2}$).

C. The use of feedback

Let us now move on to a discrimination strategy using feedback as illustrated in Fig.5. It presumes the possibility to locally access the environment [15].

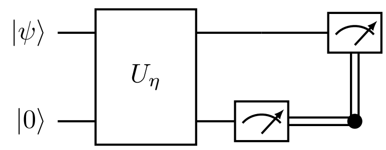

Figure 5: Channel discrimination with feedback. A first measurement is performed on the environment (bottom line), and then according to its outcome, a second measurement is performed on the system (top line). Here and in the following figures, double lines represent classical information.

We perform on the environment a measurement in the basis $\{|\alpha^+\rangle, |\alpha^-\rangle\}$, where

$$|\alpha^\pm\rangle = \cos\alpha\,|0\rangle \pm \sin\alpha\,|1\rangle \tag{21}$$

are two orthogonal states in the plane $x - z$ with $\alpha \in [0, \pi/2]$ to be determined.

Then, depending on the environment's measurement result, we choose a proper observable for the system. In this way, the feedback *actuation* has to be intended as the measurement on the main system performed conditioned to the environment's measurement outcome.

We can hence distinguish between the following possibilities:

- Environment outcome +1 (eigenvalue corresponding to $|\alpha^+\rangle$). This happens with probability:

$$\begin{aligned} P(+1) = &\frac{1}{2}\mathrm{Tr}\left(\langle\alpha^+|\,U_{\eta_0}\,|\psi\rangle\,|0\rangle\,\langle 0|\,\langle\psi|\,U_{\eta_0}^\dagger\,|\alpha^+\rangle\right) \\ &+ \frac{1}{2}\mathrm{Tr}\left(\langle\alpha^+|\,U_{\eta_1}\,|\psi\rangle\,|0\rangle\,\langle 0|\,\langle\psi|\,U_{\eta_1}^\dagger\,|\alpha^+\rangle\right), \end{aligned} \tag{22}$$

  and the resulting state on the system is

$$|\varphi_0^+\rangle = \frac{1}{N_0^+}\,\langle\alpha^+|\left(U_{\eta_0}\,|\psi\rangle\,|0\rangle\right), \tag{23}$$

  or

$$|\varphi_1^+\rangle = \frac{1}{N_1^+}\,\langle\alpha^+|\left(U_{\eta_1}\,|\psi\rangle\,|0\rangle\right), \tag{24}$$

  depending on which unitary has acted. Here, $1/N_i^+, i = 0, 1$ are normalization factors. It is then optimal to measure the observable $|\varphi_0^+\rangle\langle\varphi_0^+| - |\varphi_1^+\rangle\langle\varphi_1^+|$ on the main system to discriminate between (23) and (24) [1]. This can be done, following (15), with probability[19] $\frac{1}{2}\left(1 + \sqrt{1 - |\langle\varphi_0^+|\varphi_1^+\rangle|^2}\right)$. Thus, the probability of success when environment outcome is $+1$, reads:

$$P_{succ}^{(+)} = P(+1) \times \frac{1}{2}\left(1 + \sqrt{1 - |\langle\varphi_0^+|\varphi_1^+\rangle|^2}\right). \tag{25}$$

- Environment outcome -1 (eigenvalue corresponds to $|\alpha^-\rangle$). This happens with probability:

$$\begin{aligned} P(-1) = & \frac{1}{2}\mathrm{Tr}\left(\langle\alpha^-|\, U_{\eta_0}\,|\psi\rangle\,|0\rangle\,\langle 0|\,\langle\psi|\,U^\dagger_{\eta_0}\,|\alpha^-\rangle\right) \\ & + \frac{1}{2}\mathrm{Tr}\left(\langle\alpha^-|\, U_{\eta_1}\,|\psi\rangle\,|0\rangle\,\langle 0|\,\langle\psi|\,U^\dagger_{\eta_1}\,|\alpha^-\rangle\right), \end{aligned} \tag{26}$$

and the resulting state on the system is

$$|\varphi_0^-\rangle = \frac{1}{N_0^-}\,\langle\alpha^-|\left(U_{\eta_0}\,|\psi\rangle\,|0\rangle\right), \tag{27}$$

or

$$|\varphi_1^-\rangle = \frac{1}{N_1^-}\,\langle\alpha^-|\left(U_{\eta_1}\,|\psi\rangle\,|0\rangle\right), \tag{28}$$

depending on the acted unitary. Here $1/N_i^-, i = 0,1$ are normalization factors. It is then optimal to measure the observable $|\varphi_0^-\rangle\langle\varphi_0^-| - |\varphi_1^-\rangle\langle\varphi_1^-|$ on the main system to discriminate between (27) and (28). Thus, the probability of success when environment outcome is -1, reads:

$$P^{(-)}_{succ} = P(-1)\times\frac{1}{2}\left(1+\sqrt{1-|\langle\varphi_0^-|\varphi_1^-\rangle|^2}\right). \tag{29}$$

Finally, putting (25) and (29) together we get the overall probability of success as

$$\begin{aligned} P_{succ} &= P^{(+)}_{succ} + P^{(-)}_{succ} \\ &= \frac{\chi}{2}\left[1+\sin\alpha\sin\left(\frac{\eta_0-\eta_1}{2}\right)\sqrt{\frac{x\,(\mu+\nu)}{c_1c_2}}\right] \\ &+ \frac{1-\chi}{2}\left[1+\cos\alpha\sin\left(\frac{\eta_0-\eta_1}{2}\right)\sqrt{\frac{x\,(\mu-\nu)}{(1-c_1)(1-c_2)}}\right], \end{aligned} \tag{30}$$

where

$$\chi \equiv \frac{1}{2} - \frac{1}{2}\cos(2\alpha)\left[1 - x\left(\sin^2\eta_0 + \sin^2\eta_1\right)\right], \tag{31a}$$

$$\mu \equiv \left[1 + (2x-1)\cos\eta_0\cos\eta_1 + \sin\eta_0\sin\eta_1\right], \tag{31b}$$

$$\nu \equiv \cos(2\alpha)\left[(2x-1) + \cos\eta_0\cos\eta_1 + (2x-1)\sin\eta_0\sin\eta_1\right], \tag{31c}$$

$$c_i \equiv \frac{1}{2} - \frac{1}{2}\cos(2\alpha)\left[1 - 2x\sin^2\eta_i\right], \qquad i = 0,1. \tag{31d}$$

Analyzing Eq.(30), we found the maximum success probability as

$$P_{succ} = \frac{1+\sin(\eta_0-\eta_1)}{2}, \tag{32}$$

attained when $x = 1$ and $\alpha = \frac{\pi}{4}$. Provided that $\eta_0 \neq \eta_1$ and $\eta_0 \neq \frac{\pi}{2} - \eta_1$, we have the probability of success with feedback greater than without feedback as shown in Fig.6.

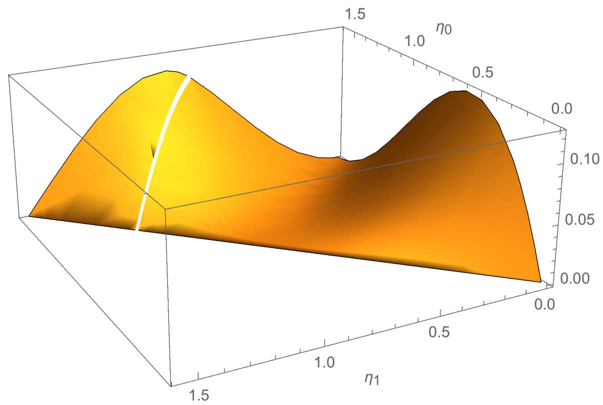

Figure 6: Difference between the maximum probability of success with feedback (32) and without feedback (17) vs η_0 and η_1. The white line corresponds to $\gamma = 1/\sqrt{2}$ (see (12)).

We note that the best measurement on the environment is on the basis $|\pm\rangle \equiv (|0\rangle \pm |1\rangle)/\sqrt{2}$ and the best input state is always $|1\rangle$ in contrast to what happened in the absence of feedback. In Fig.6 it is also visible a slight asymmetry of the behavior with respect to η_0 and η_1.

Finally, it is worth mentioning a similarity of this problem with the discrimination of unitary dilations of the amplitude damping channel using local measurements (analogous similarity was pointed out in Ref.[17] for channel estimation).

III. TWO-SHOT DISCRIMINATION

In this section, we shall consider the discrimination assuming to have two copies of the channel characterized either by parameter η_0 or by parameter η_1 (with again equal probability $1/2$).

A. Optimal input

Let us first consider the possibility of using entangled inputs. Since for a single shot the optimal input state lies in the $x-z$ plane, we construct entangled input states as a linear combination of 2-fold tensor product of these states with real coefficients. This amounts to consider the two inputs state as

$$\sqrt{1-x}|01\rangle + \sqrt{x}|10\rangle, \tag{33}$$

or

$$\sqrt{1-x}|00\rangle + \sqrt{x}|11\rangle, \tag{34}$$

with $x \in [0,1]$.

According to the 2-fold action of (4), in case of (33) we will get the output states as

$$\begin{aligned}\rho_i^{(2)} &= \sin^2\eta_i|00\rangle\langle 00| + (1-x)\cos^2\eta_i|01\rangle\langle 01| + x\cos^2\eta_i|10\rangle\langle 10| \\ &\quad + \sqrt{x(1-x)}\cos^2\eta_i\left(|01\rangle\langle 10| + |10\rangle\langle 01|\right), \quad i=0,1.\end{aligned} \tag{35}$$

While in case of (34) as

$$\begin{aligned}\rho_i^{(2)} &= \left((1-x) + x\sin^4\eta_i\right)\eta|00\rangle\langle 00| + x\sin^2\eta_i\cos^2\eta_i\left(|01\rangle\langle 01| + |10\rangle\langle 10|\right) + x\cos^4\eta_i|11\rangle\langle 11| \\ &\quad + \sqrt{x(1-x)}\cos^2\eta_i\left(|00\rangle\langle 11| + |11\rangle\langle 00|\right), \quad i=0,1.\end{aligned} \tag{36}$$

Using (15) with the states (35) gives

$$P_{succ} = \frac{1}{2}\left(1 + \sin^2\eta_0 - \sin^2\eta_1\right), \tag{37}$$

which is independent of x. On the other hand, using (15) with the states (36) gives

$$P_{succ} = \frac{1}{32}\Bigg\{16 + 4x\left|\cos^2(2\eta_0) - \cos^2(2\eta_1)\right| + 4\sqrt{2}x\left(\cos^2\eta_1 - \cos^2\eta_0\right)\left[4 - x\left(\cos(2\eta_0) + \cos(2\eta_1)\right)^2\right]\Bigg\}, \tag{38}$$

which attains its maximum for $x = 1$. Therefore, we can conclude that entanglement across the two inputs is useless. Then, we consider as input the 2-fold tensor product of (7) and optimize over x. In other words, we consider

$$P_{succ} = \max_x \frac{1}{2}\left(1 + \frac{1}{2}\left\|\rho_0\otimes\rho_0 - \rho_1\otimes\rho_1\right\|_1\right), \tag{39}$$

where ρ_is are given by (9).

The difference between this optimized success probability and (17) is shown in Fig.7.

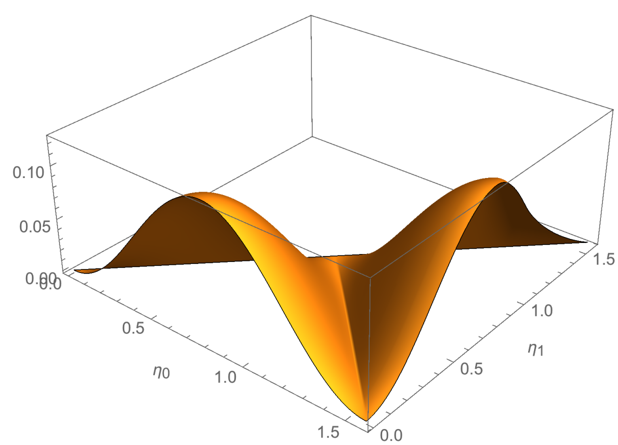

Figure 7: Difference between the maximum probability of success (39) and (17) vs η_0 and η_1.

The optimal value x^* of x for (39) as function of η_0 and η_1 is reported in Fig.8. Note that the region where the x^* value is smaller than one is shrunk with respect to the single-shot case ($\gamma < 1/2$). Although the exact boundary cannot be expressed analytically, the following bound holds:

$$\gamma(\eta_0, \eta_1) < \frac{1}{2} \Rightarrow x < 1, \tag{40}$$

where $\gamma(\eta_0, \eta_1)$ is given by (12). It is worth remarking that for $x^* = 1$ the optimal observable $\rho_0 - \rho_1$ constructed with (35) turns out to be local (its normalized eigenvectors are $|00\rangle, |01\rangle, |10\rangle, |11\rangle$), while for $x^* < 1$ results nonlocal (its normalized eigenvectors are entangled).

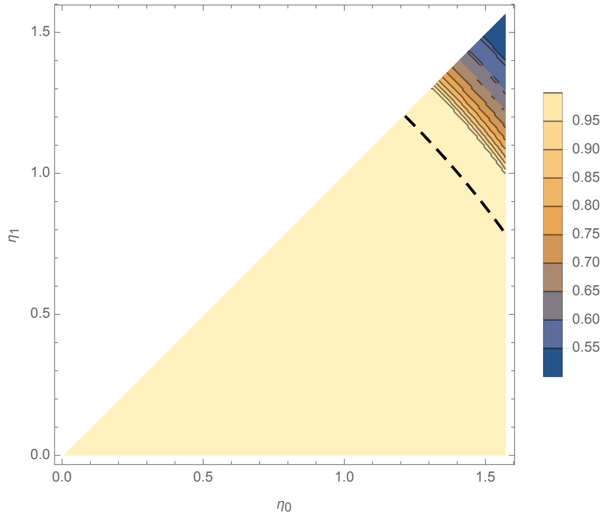

Figure 8: Optimal value x^* of x for (39) vs η_0 and η_1. The black dashed line represents the boundary $\gamma = 1/\sqrt{2}$ for the single-shot case.

B. Adaptive strategy

In the previous subsection, although getting rid of entangled inputs, we saw the necessity of using collective measurement in some parts of the parameters' region. What happens if we restrict to individual measurements to have a completely local strategy (analogoulsy to [16])? We expect an improvement with respect to the one shot-case, but this relies on using an adaptive strategy, which can generally be depicted as in Fig.9.

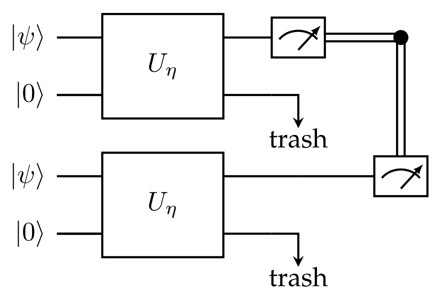

Figure 9: Schematic representation of channel discrimination through a local adaptive strategy. The measurement outcome on the first copy determines the measurement to be performed on the second copy.

At the output of the two channel copies, we have

$$\frac{1}{2}\rho_0^{\otimes 2} + \frac{1}{2}\rho_1^{\otimes 2}, \tag{41}$$

with ρ_i given by (9).

On the first copy we use the POVM whose elements are $|v_0\rangle\langle v_0|$ and $|v_1\rangle\langle v_1|$, with $|v_0\rangle$ and $|v_1\rangle$ the (normalized) eigenvectors of the observable $\rho_0 - \rho_1$. On the second copy, we choose a POVM depending on the previous copy's measurement outcome, i.e., $\Pi_{x_2}^{x_1}$, $x_i \in \{0, 1\}$, where the subscript denotes the element of the POVM, while the superscript the dependence from the previous measurement outcome. We define

$$P_j(x_2|x_1) \equiv \mathrm{Tr}\left[\rho_j \Pi_{x_2}^{x_1}\right] . \tag{42}$$

Then the success probability will be given by

$$\begin{aligned} P_{succ} = &\frac{1}{2}\left[P_0(0|0)\langle v_0|\rho_0|v_0\rangle + P_0(0|1)\left(1-\langle v_0|\rho_0|v_0\rangle\right)\right] \\ &+ \frac{1}{2}\left[P_1(1|1)\langle v_1|\rho_1|v_1\rangle + P_1(1|0)\left(1-\langle v_1|\rho_1|v_1\rangle\right)\right] . \end{aligned} \tag{43}$$

Eq.(43) should be maximized overall POVMs $\Pi_{x_2}^{x_1}$. Actually, the first and fourth terms can be maximized overall Π_0^0 being $\Pi_1^0 = I - \Pi_0^0$, while the second and third terms can be maximized overall Π_1^1 being $\Pi_0^1 = I - \Pi_1^1$.

So we can independently perform the following maximizations (for fixed input x):

$$\begin{aligned} &\max_{\Pi_0^0: 0\le \Pi_0^0 \le I} \frac{1}{2}\left[P_0(0|0)\langle v_0|\rho_0|v_0\rangle + P_1(1|0)\left(1-\langle v_1|\rho_1|v_1\rangle\right)\right] \\ = &\max_{\Pi_0^0: 0\le \Pi_0^0 \le I} \frac{1}{2}\left\{\mathrm{Tr}\left[\rho_0\Pi_0^0\right]\langle v_0|\rho_0|v_0\rangle + \mathrm{Tr}\left[\rho_1(I-\Pi_0^0)\right]\left(1-\langle v_1|\rho_1|v_1\rangle\right)\right\} , \end{aligned} \tag{44}$$

and

$$\begin{aligned} &\max_{\Pi_1^1: 0\le \Pi_1^1 \le I} \frac{1}{2}\left[P_1(1|1)\langle v_1|\rho_1|v_1\rangle + P_0(0|1)\left(1-\langle v_0|\rho_0|v_0\rangle\right)\right] \\ = &\max_{\Pi_1^1: 0\le \Pi_1^1 \le I} \frac{1}{2}\left\{\mathrm{Tr}\left[\rho_1\Pi_1^1\right]\langle v_1|\rho_1|v_1\rangle + \mathrm{Tr}\left[\rho_0(I-\Pi_1^1)\right]\left(1-\langle v_0|\rho_0|v_0\rangle\right)\right\} . \end{aligned} \tag{45}$$

The 2×2 matrices Π_0^0 and Π_1^1 providing this maxima can be found as in Appendix A. From them, we will get the success probability as a function $P_{succ}(\eta_0, \eta_1, x)$.

To evaluate the performance of the adaptive strategy, we compare this probability, maximized over x, with the optimal success probability for two-shot (39). Fig.10 shows the difference between the latter and the former. As we expected, such a difference is nonzero only in the region of Fig.8 where $x^* < 1$, however it is very tiny. This shows that the devised local adaptive strategy performs almost like the strategy involving collective measurement.

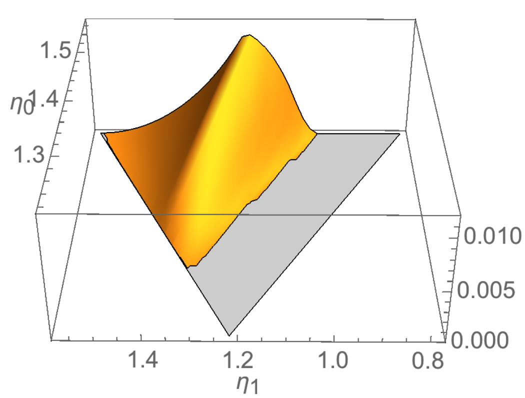

Figure 10: Difference between the maximum probability of success using collective measurement and that using the adaptive strategy vs η_0 and η_1 in the region $\gamma < 1/\sqrt{2}$.

Furthermore, Fig.11 shows the difference between the maximum probability of success using using the adaptive strategy and that of a single-shot. Note that the range of Fig.11 is one order of magnitude bigger than Fig.10.

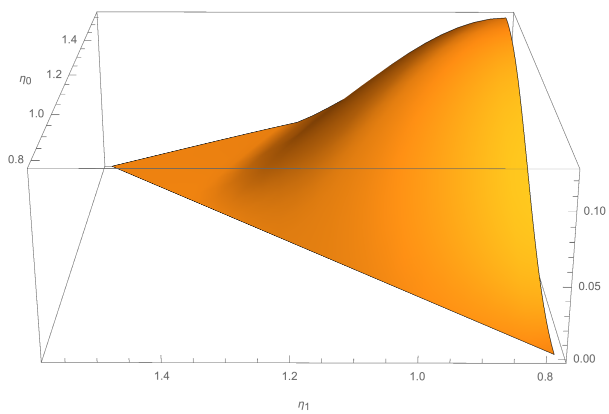

Figure 11: Difference between the maximum probability of success using using the adaptive strategy and that of a single shot vs η_0 and η_1.

C. Adaptive strategy with feedback

We now develop an adaptive strategy that includes the feedback from the environment, as illustrated in Fig.12.

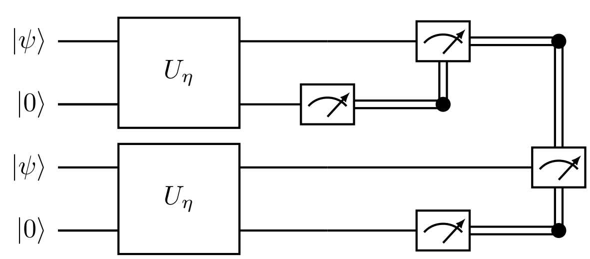

Figure 12: Schematic representation of channel discrimination through a local adaptive strategy including feedback. On each step the measurement to be performed on the main system is determined by the measurement outcome of the environment on that step, together with the measurement outcome of the main system at the previous step.

On the first copy of the unitary, we proceed like in Subsection II C, defining a POVM $\Pi^{e_1}_{x_1}$ whose elements are

$$\Pi^{e_1}_{x_1=0} = |v^{e_1}_0\rangle\langle v^{e_1}_0|, \tag{46}$$
$$\Pi^{e_1}_{x_1=1} = |v^{e_1}_1\rangle\langle v^{e_1}_1|, \tag{47}$$

where $|v^{e_1}_0\rangle$ and $|v^{e_1}_1\rangle$ are (normalized) eigenvectors of $\varphi^{e_1}_0 - \varphi^{e_1}_1$. Here $\varphi^{e_1}_j \equiv |\varphi^{e_1}_j\rangle\langle\varphi^{e_1}_j|$ with $j = 0, 1$ and $e_1 = \pm$. Note that following the conclusions of Subsection II C, we are considering the input $|\psi\rangle$ as $|1\rangle$ and the measurement on the environment on the basis $|\pm\rangle$, so that

$$|\varphi_0^{\pm}\rangle = \mp i \sin\eta_0|0\rangle + \cos\eta_0|1\rangle, \tag{48a}$$
$$|\varphi_1^{\pm}\rangle = \mp i \sin\eta_1|0\rangle + \cos\eta_1|1\rangle. \tag{48b}$$

As a consequence, at the output of the main system, we have to distinguish between pure states (differently to what happened in the previous Subsection). Therefore, on the second copy of the unitary it would be optimal to perform a measurement that confirms or disproves the outcome of the first shot. This is realized choosing POVMs whose elements are

$$\Pi_{x_2=x_1}^{x_1,\,e_2} = |\varphi_{x_1}^{e_2}\rangle\langle\varphi_{x_1}^{e_2}|, \tag{49a}$$
$$\Pi_{x_2=x_1\oplus 1}^{x_1,\,e_2} = \left|\left(\varphi_{x_1}^{e_2}\right)^{\perp}\right\rangle\left\langle\left(\varphi_{x_1}^{e_2}\right)^{\perp}\right|, \tag{49b}$$

where $x_i \in \{0,1\}$ and $e_2 = \pm$. Again the superscript denotes conditioning (to the outcome of the previous shot and the environment's measurement).

We then define the probability

$$P_j^{e_2}(x_2|x_1,e_2) \equiv \mathrm{Tr}\left[\varphi_j^{e_2}\,\Pi_{x_2}^{x_1,\,e_2}\right]. \tag{50}$$

In terms of it, we can express the success probability as

$$P_{succ} = \sum_{e_1,e_2=\pm}\frac{1}{8}\Big[P_0^{e_2}(0|0,e_2)\langle v_0^{e_1}|\varphi_0^{e_1}|v_0^{e_1}\rangle + P_0^{e_2}(0|1,e_2)\left(1-\langle v_0^{e_1}|\varphi_0^{e_1}|v_0^{e_1}\rangle\right)$$
$$+ P_1^{e_2}(1|1,e_2)\langle v_1^{e_1}|\varphi_1^{e_1}|v_1^{e_1}\rangle + P_1^{e_2}(1|0,e_2)\left(1-\langle v_1^{e_1}|\varphi_1^{e_1}|v_1^{e_1}\rangle\right)\Big], \tag{51}$$

where the factor $\frac{1}{8}$ in front of the square brackets arises from the probability $\frac{1}{2}$ of having $U_{\eta_i}\otimes U_{\eta_i}$, the probability $\frac{1}{2}$ for e_1 to take one of the two values, and the probability $\frac{1}{2}$ for e_2 to take one of the two values. Computing explicitly (50) we arrive at

$$P_{succ} = \frac{1+\sin(\eta_0-\eta_1)}{2} + \frac{1-\sin(\eta_0-\eta_1)}{2}\sin^2(\eta_0-\eta_1). \tag{52}$$

The improvement with respect to the single-shot with feedback (Eq.(32)) is shown in Fig.13. We can see that it is positive in all parameters' region (but $\eta_1 = \eta_0$ and $\eta_0 = \frac{\pi}{2}, \eta_1 = 0$) and is maximum for $\eta_1 = \eta_0 - \frac{\pi}{4}$.

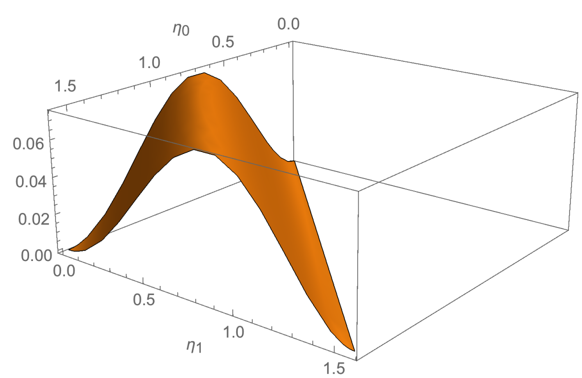

Figure 13: Difference between the probabilities of success (52) and (32) vs η_0 and η_1.

IV. CONCLUDING REMARKS

We have addressed the issue of discriminating between two-qubit amplitude damping channels by considering single and double-shot. For the one-shot, we showed that the excited state as input is not always optimal, and the side entanglement assistance has a limited benefit. In contrast, feedback assistance from the environment is highly beneficial. About feedback, we suspect that it will be even more effective in case of discrimination of random unitary channels, where the information recovered from the environment neutralizes the channel action (taking it back to identity map).

For the two-shot, we proved the in-utility of entangled inputs. Then, focusing on individual (local) measurements, we found the optimal adaptive strategy. We are confident that this strategy can be extended in a Markovian way to n-shot, and the asymptotic analysis of its performance would be foreseeable. Similarly, the adaptive strategy is applied to environment feedback assisted discrimination showing a smaller improvement than the case without feedback (cfr. Figs.11 and 13). This is because feedback has provided a big enhancement already on the first shot.

In the future, it is worth extending the performed analysis to d-dimensional amplitude damping channels, also with restrictions on the set of input states (e.g., energy restriction). After all, investigating amplitude damping channel discrimination in discrete systems can also provide new insights for distinguishing continuous variable lossy channels [18].

Appendix A: Optimal POVMs for local adaptive strategy

The qubit states of interest (Eq.(9)) can be compactly written as

$$\rho_i = \begin{pmatrix} r_i & s_i \\ s_i & 1-r_i \end{pmatrix}, \quad j=0,1. \tag{A1}$$

Since they are located in the $x-z$ plane, we can consider, without loss of generality, the POVM element Π_0^0 (or analogously Π_1^1) as

$$\begin{pmatrix} a & b \\ b & c \end{pmatrix}, \qquad I - \begin{pmatrix} a & b \\ b & c \end{pmatrix}, \tag{A2}$$

with $a,b,c \in \mathbb{R}$ such that $0 \leq \begin{pmatrix} a & b \\ b & c \end{pmatrix} \leq I$. Then, Eq.(44) (or analogously Eq.(45)) can be cast into the form

$$\begin{aligned}\max_{\left\{a,b,c\in\mathbb{R}\,:\,0\leq\begin{pmatrix} a & b \\ b & c \end{pmatrix}\leq I\right\}} & \Big\{\frac{1}{2}\left[r_0\langle v_0|\rho_0|v_0\rangle - r_1(1-\langle v_1|\rho_1|v_1\rangle)\right]a \\ & + \left[s_0\langle v_0|\rho_0|v_0\rangle - s_1(1-\langle v_1|\rho_1|v_1\rangle)\right]b \\ & + \frac{1}{2}\left[(1-r_0)\langle v_0|\rho_0|v_0\rangle - (1-r_1)(1-\langle v_1|\rho_1|v_1\rangle)\right]c \\ & + \frac{1}{2}(1-\langle v_1|\rho_1|v_1\rangle)\Big\}.\end{aligned} \tag{A3}$$

This is equivalent to

$$\max_{\left\{a,b,c\in\mathbb{R}\,:\,0\leq\begin{pmatrix} a & b \\ b & c \end{pmatrix}\leq I\right\}} Aa + Bb + Cc, \tag{A4}$$

with $A, B, C \in \mathbb{R}$.

First, we note that the condition $0 \leq \begin{pmatrix} a & b \\ b & c \end{pmatrix} \leq I$ is equivalent to the conditions **C1)** or **C2)** or **C3)** listed below:

C1) $(a = 0 \vee a = 1) \wedge (b = 0) \wedge (0 \leq c \leq 1)$;

C2) $(0 < a < 1) \wedge \left(b = -\sqrt{a - a^2} \vee b = +\sqrt{a - a^2}\right) \wedge \left(c = 1 + \frac{b^2}{-1+a}\right)$;

C3) $(0 < a < 1) \wedge \left(-\sqrt{a - a^2} < b < +\sqrt{a - a^2}\right) \wedge \left(\frac{b^2}{a} \leq c \leq 1 + \frac{b^2}{-1+a}\right)$.

Second, we note that to find (A4) it would be enough to multiply each positive (resp. negative) coefficient by the maximum (resp. minimum) value of the corresponding variable. Let us then analyze all possible cases.

i) According to **C1)**, we can have the following maxima

$$
\begin{aligned}
0 \quad & \text{with } a = c = 0, \quad \text{when } A, B, C < 0, && \text{(A5)} \\
A \quad & \text{with } a = 1,\ c = 0, \quad \text{when } A > 0, C < 0, && \text{(A6)} \\
C \quad & \text{with } a = 0,\ c = 1 \quad \text{when } A < 0, C > 0, && \text{(A7)} \\
A + C \quad & \text{with } a = c = 1, \quad \text{when } A, C > 0. && \text{(A8)}
\end{aligned}
$$

ii) According to **C2)**, we can set $b = \mathrm{sign}(B)\sqrt{a - a^2}$ and $c = 1 + \frac{b^2}{a-1} = 1 - a$, and then maximize over a obtaining

$$
\frac{1}{2}\left[A + C + \frac{B^2 + (A - C)^2}{\sqrt{B^2 + (A - C)^2}}\right], \tag{A9}
$$

$$
\frac{1}{2}\left[A + C + \frac{B^2 - (A - C)^2}{\sqrt{B^2 + (A - C)^2}}\right], \tag{A10}
$$

where the first refers to $A > C$, and the second to $A < C$. Such maxima are attained when $a = \frac{1}{2}\left[1 \pm \frac{|A-C|}{\sqrt{B^2+(A-C)^2}}\right]$.

iii) According to **C3)** we can set $c = \frac{b^2}{a}$ or $c = 1 + \frac{b^2}{-1+a}$, and then maximize over a and b. However, this leads to $a = 0$ or $a = 1$ which is not consistent with the requirement of **C3)**.

Summarizing, the problem (A4) can be solved by taking the greatest value among (A5)-(A10).

The authors equally contributed to this work.

The work was financially supported by the Future and Emerging Technologies (FET) programme, within the Horizon-2020 Programme of the European Commission, under the FET-Open grant agreement QUARTET, number 862644.

The authors thank Francisco Revson F. Pereira for useful discussions.

---

[1] S. Mancini, and A. Winter, *A Quantum Leap in Information Theory*, World Scientific (2020).

[2] A. Acin, *Statistical distinguishability between unitary operations*, Physical Review Letters, **87**, 177901 (2001).

[3] A. Gilchrist, N. K. Langford, and M. A. Nielsen, *Distance measures to compare real and ideal quantum processes*, Physical Review A **71**, 062310 (2005).

[4] M. Sacchi, *Optimal discrimination of quantum operations*, Physical Review A **71**, 062340 (2005).

[5] G. Wang, and M. Ying, *Unambiguous discrimination among quantum operations*, Physical Review A **73**, 042301 (2006).

[6] M. Hayashi, *Discrimination of two channels by adaptive methods and its application to quantum system*, IEEE Transactions on Information Theory **55**, 3807 (2009).

[7] A. M. Childs, J. Preskill, and J. Renes, *Quantum information and precision measurement*, Journal of Modern Optics, **47**, 155-176 (2000).

[8] B. Rosgen, and J. Watrous, *On the hardness of distinguishing mixed-state quantum computations*, Proceedings of the 20th IEEE Conference on Computational Complexity, pp. 344-354 (2005).

[9] M. Sacchi, *Entanglement can enhance the distinguishability of entanglement-breaking channels*, Physical Review A **72**, 014305 (2005).

[10] M. Sacchi, *Minimum error discrimination of Pauli channels*, Journal of Optics B: Quantum and Semiclassical Optics **7**, S333 (2005).

[11] C. W. Helstrom, *Quantum detection and estimation theory*, Journal of Statistical Physics, **1**, 231-252 (1969).

[12] A. S. Holevo, *Statistical decision theory for quantum systems*, Journal of Multivariate Analysis **3**, 337-394 (1973).

[13] S. Pirandola, R. Laurenza, C. Lupo, and J. L. Pereira, *Fundamental limits to quantum channel discrimination*, arXiv:1803.02834 (2019).

[14] V. Katariya, and M. M. Wilde, *Evaluating the advantage of adaptive strategies for quantum channel distinguishability*, arXiv:2001.05376 (2020).

[15] L. Memarzadeh, C. Cafaro, and S. Mancini, *Quantum information reclaiming after amplitude damping*, Journal of Physics A: Mathematical and Theoretical **44**, 045304 (2011).

[16] P. Tej, S. R. Ahmed, A. R. Usha Devi, and A. K. Rajagopal, *Quantum hypothesis testing and state discrimination*, arXiv:1803.04944 (2018).

[17] M. Rexiti, and S. Mancini, *Adversarial versus cooperative quantum estimation*, Quantum Information Processing **18**, 102 (2019).

[18] C. Invernizzi, M. G. A. Paris, and S. Pirandola, *Optimal detection of losses by thermal probes*, Physical Review A **84**, 022334 (2011).

[19] This expression derives from (15) when employing pure state vectors.